

Study of Oscillations and Pattern Formation in the NO + CO Reaction on Pt(100) Surfaces through Dynamic Monte Carlo Simulation: Toward a Realistic Model

S. J. Alas[†] and G. Zgrablich^{*,‡}

Departamento de Química, Universidad Autónoma Metropolitana, Iztapalapa, P.O. Box 55-534, México D. F., México, and Laboratorio de Ciencias de Superficies y Medios Porosos, Universidad Nacional de San Luis, 5700 San Luis, Argentina

Received: February 7, 2006; In Final Form: March 29, 2006

Oscillations and pattern formation driven by a surface reconstruction are studied for the catalytic reduction of NO by CO on Pt(100) single-crystal surfaces through dynamic Monte Carlo simulations at low pressure and relatively high temperatures conditions. This study incorporates recent experimental evidence obtained for the same reaction on a Rh(111) surface, which modifies the reaction scheme used in previous approaches. The main consequence of such experimental evidence is that the production of N₂ occurs through two parallel mechanisms: (a) the classical N + N recombination step; (b) the formation and subsequent decay of an (N–NO)* intermediate species as the fastest pathway. Moreover, different factors influencing the NO dissociation rate, the key step in the whole reaction, such as the availability of neighboring vacant sites, the formation of N-islands, and the presence of other NO and CO adsorbed species in the neighborhood, are also taken into account and their effects discussed. Sustained, modulated, irregular, and damped oscillations are observed in our analysis as well as the formation of cellular structures and turbulent patterns. The effect and the importance of each elementary reaction step on the behavior of the system are discussed.

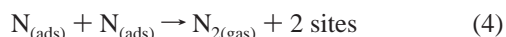
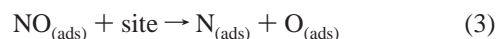
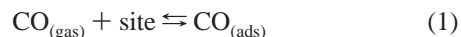
1. Introduction

The catalytic NO + CO reaction on metals has received a great deal of attention for a long time in the literature, both from experimental and from theoretical points of view, due to its importance in the problem of atmospheric pollution control. In addition to this importance, there is an intrinsic fundamental interest, given that this monomer–dimer reaction, i.e., a reaction involving a particle adsorbing on one site and a particle adsorbing and dissociating on two sites, presents nonlinear phenomena like kinetic oscillations and spatiotemporal pattern formation.^{1–14}

A variety of catalyzed reactions have been found to show oscillatory behavior under nearly real conditions, i.e., polycrystalline surfaces or supported catalysts at relatively high pressures.⁵ Under these conditions, reactions are typically nonisothermal and many effects contribute to obscure the delicate interplay between elementary steps leading to complex behavior. Experimental studies of catalytic reactions on single crystals under isothermal conditions at low pressures have provided valuable information that can be used to develop and evaluate theoretical models based on the microscopic properties of the system. However, these studies have been concerned with only a narrow range of catalytic reactions, mainly CO oxidation on Pt and Pd surfaces and NO reduction by several agents (CO, H₂, and NH₃) on Pt(100) and Rh(110).⁵ It is well-known that the (100) and (110) faces of noble metals undergo a surface reconstruction driven by adsorbed molecules during these reactions, and this phenomenon is an important ingredient in the appearance of the oscillatory behavior.

Oscillations and spatiotemporal patterns have particularly been observed for the NO + CO reaction on the Pt(100) surface under isothermal, low-pressure conditions ($p \sim 10^{-6}$ – 10^{-4} Pa).^{1–6} It is well-known that the clean Pt(100) surface at $T >$

420 K exhibits a quasi-hexagonal configuration (hex) of the atoms in the topmost layer, but surface reconstruction can take place by the uptake of adsorbates such as CO and NO then leading to the formation of a (1 × 1) square structure.^{2–8} The lifting of this surface reconstruction can take place when a reconstructed site becomes empty. This constitutes an adsorbate-induced hex \rightleftharpoons 1 × 1 surface phase transition, which, at $T >$ 450 K, is directly involved in the formation of oscillations during the course of the NO + CO reaction.^{2–11} Another fundamental ingredient, necessary for the observation of kinetic oscillations and spatiotemporal patterns, is a synchronization mechanism, such that the contributions of different local oscillators do not average out to a stationary reaction rate. In controlled isothermal and low pressure conditions the mechanism leading to this synchronization is the surface diffusion of reactants. A relatively fast surface diffusion of some of the reactants is necessary in order to correlate what is going on in the reaction at relatively distant surface positions.¹ The typical mechanism of NO reduction by CO on the Pt(100) surface that has been traditionally assumed in the literature consists of the following sequence of reaction steps:



In one of these reaction steps, we can observe that the production of N_{2(gas)} occurs through the recombination of two N atoms adsorbed at two nearest-neighbor (nn) sites. The

* Corresponding author. E-mail: giorgio@unsl.edu.ar.

[†] Universidad Autónoma Metropolitana.

[‡] Universidad Nacional de San Luis.

formation of the products of this reaction is directly related to the rate of NO dissociation; moreover, such dissociation can only occur on the square 1×1 phase, since it is quite insignificant on the hex phase of the Pt(100) surface, as it has been reported in previous studies.^{4,6,10}

The above reaction mechanism has also been accepted for the same reaction taking place over the Rh(111) surface.¹⁵ Nevertheless, molecular beam experiments on the reduction of NO over Rh(111)^{16–22} have indicated that the standard reaction scheme used to explain the kinetics of this reaction needs to be modified in at least two important ways. First, it was found that when a ¹⁴N-covered Rh(111) surface is exposed to a ¹⁵NO + CO beam, the majority of molecular nitrogen produced contains at least one ¹⁵N atom.^{16–18} This means that the nitrogen recombination step, $N(\text{ads}) + N(\text{ads}) \rightarrow N_2(\text{gas}) + 2 \text{ sites}$, usually assumed to be responsible for the formation of molecular nitrogen is in fact not fast enough under typical reaction conditions to account for the N_2 production rate. Instead, an intermediate species, $(N-NO)^*$, appears to form on the surface and then either decomposes to $N_2(\text{gas}) + O(\text{ads})$ or just simply desorbs. In a realistic description of the reaction, both the nitrogen recombination step and the formation of the $(N-NO)^*$ intermediary should be considered in parallel, the last one being the predominant step.^{22,23} A second important modification to the NO reduction mechanism brought about by the molecular beam work arises from the evidence that, at least on Rh(111) surfaces, atomic N forms compact islands. Indeed, it was found that the isotopic distribution of the molecular nitrogen detected in temperature-programmed desorption (TPD) spectra from surfaces prepared by using isotopic mixtures of ¹⁴N- and ¹⁵N-labeled nitrogen oxide can only be explained on that basis.^{19,21} The mechanism for the formation of these islands, however, has not yet been established.

It has already been suggested^{24,25} that the alternative reaction mechanism observed for Rh(111) could be valid also for other surfaces like, for example, Rh(100) or Pt(100) where the hex $\rightleftharpoons 1 \times 1$ phase reconstruction takes place. Although there is no direct experimental evidence for the occurrence of this mechanism on Pt(100) or Rh(100), it is also true that there is no direct experimental evidence for the contrary. The production of N_2 via a parallel NO + N recombination step has been considered by several authors in the literature. For example, Kortlüke et al.²⁶ assume the recombination step in studying the reaction on polycrystalline Rh; Cho²⁷ proposed a mechanism where N_2 is produced via the formation of a surface N_2O species, whose formation was demonstrated by early studies for Rh supported on silica²⁸ and by early TPD studies on Rh(111) by the General Motors group. The arguments in favor of the alternative reaction mechanism can be reinforced by the DFT calculations developed by Neurock et al.^{29,30} on NO dissociation and other related processes on Pt(100). In fact, they show that the activation energy for NO dissociation is 107.1 kJ/mol, that for the inverse reaction is 21.0 kJ/mol, that for the N + N recombination step is 9.0 kJ/mol, that for the formation of N_2O from adsorbed N and NO is 141.9 kJ/mol, and that for the N_2O decay to $N_2(\text{gas})$ is 0.0 kJ/mol. Considering that two NO must dissociate for the N + N reaction pathway, while only one is needed for the NO + N pathway and that the activation energy for the recombination of NO from N and O is small compared to the activation energy for NO desorption (214.3 kJ/mol), which enhances the probability of finding undissociated NO on the surface, it is then reasonable to assume that both pathways may contribute to the overall reaction mechanism.

On the other hand, Fink et al. found experimentally that NO dissociation is inhibited by the presence of neighboring coadsorbed NO or CO species in the NO + CO reaction on the Pt(100) surface.^{9,10} While Niemantsverdriet and co-workers observed the same effect in the same reaction on the Rh(111) surface, they also detected that NO dissociation is facilitated by the existence of several vacant sites.³¹ The inhibition effect on NO dissociation is of fundamental importance. In fact it was shown to be absolutely necessary in order to explain the negligible O coverage observed experimentally at steady state for low CO concentrations in the gas phase.²³

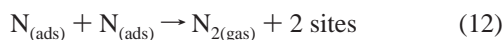
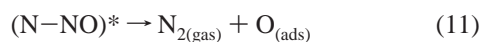
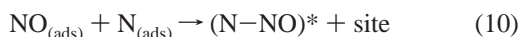
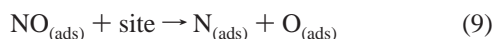
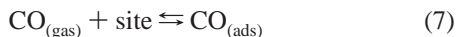
It is therefore natural, to advance toward a realistic model for this reaction, to incorporate the above information emerging from the mentioned experimental studies into the reaction scheme and evaluate the effects of each factor. Given that the slow step of the catalyzed NO + CO reaction is NO dissociation, the possibility of N_2 production through both the formation of the $(N-NO)^*$ intermediary and the formation of the classical N + N recombination, as well as the formation of N-islands and the inhibition effect on NO dissociation by coadsorbed NO or CO, should produce relevant differences in the conditions under which oscillations and pattern formation appear. It is our purpose here to determine these conditions.

Previous studies^{24,25} have incorporated only partially some of the above features in the modified reaction scheme, with encouraging results. In particular, it was assumed that the formation of the $(N-NO)^*$ intermediate was the only reaction pathway for N_2 production. However, the inclusion of the N + N alternative pathway, even though slower, was shown to help to reproduce observed O and N steady-state coverage over the whole range of CO concentrations in the gas phase.²³ The fundamental inhibition effect on NO dissociation was not included into those studies, and neither was the formation of N-islands, although the latter is expected to be of smaller importance, as we shall see later, due to the fact that N is rapidly removed from the surface. Nevertheless, they provided the necessary background to attempt a more complete model. Accordingly, the purpose of the present work is to extend the previous studies by incorporating into the reaction scheme all the experimental information available so far.

Dynamic Monte Carlo simulations, from which the behavior of the catalytic system can be simulated in real time units,³² will be used in the calculations. Specifically, we will apply the above dynamic simulation technique to the NO + CO reaction on a Pt(100) surface by considering alternative steps in the reaction mechanism taking into account the experimental findings of Zaera et al., i.e., the production of N_2 via the $(N-NO)^*$ and N + N pathways and the formation of N-islands, as well as the contributions to the NO dissociation by Fink et al. and Niemantsverdriet et al. We will discuss under which conditions a series of different oscillatory and spatiotemporal behavior can be observed and identify which are the dominant physicochemical processes that determine the occurrence of such dynamic patterns. In section 2, the model and simulation method are described. Results are presented and discussed in section 3. Finally, conclusions are given in section 4.

2. Model and Simulation Method

For the dynamic analysis of the reduction of NO by CO on a Pt(100) surface, the following general reaction scheme, which includes the new alternative steps and effects brought about by the available experimental and theoretical evidence,^{9,10,16–23,31} is assumed



Here $(\text{N}-\text{NO})^*$ is the activated complex intermediate, which eventually decays mainly to N_2 . In this reaction scheme, it can be observed that we have included the conventional $\text{N} + \text{N}$ recombination step and an alternative step involving the formation of the $(\text{N}-\text{NO})^*$ species for the production of N_2 . The former is the slower pathway and, according to ref 22, it will be given a relative probability of 0.3, while that for the $(\text{N}-\text{NO})^*$ pathway will be 0.7. Inhibition effects on NO dissociation by the presence of other coadsorbed CO and NO molecules and the formation of N-islands will be appropriately taken into account below when the NO dissociation rate will be determined. In addition to the above reaction mechanism we also consider that diffusion of adsorbed NO and CO species can take place on any of the two substrate phases as well as across phase boundaries. It is important to stress that NO dissociation can only take place on the 1×1 phase, while all other processes can take place on both the hex and the 1×1 phases.

To construct a relatively simple and manageable reaction scheme, we incorporate the following additional assumptions in devising our surface reaction mechanism:

(i) The production of N_2O is not taken into account given that the rate of this reaction is expected to be low compared to CO_2 and N_2 production.^{2,6,11}

(ii) The difference in densities between Pt atoms in the hexagonal and in the 1×1 phases is ignored, although the Pt(100) surface presents different site densities for the hexagonal and the 1×1 phases, the difference being approximately 20%.⁶

(iii) Lateral interactions among different ad-species occurring on both phases are not considered, even if these interactions have been made evident by experimental studies through $c(2 \times 2)$ and $c(2 \times 4)$ rearrangements effects.^{10,33–36}

(iv) O desorption is neglected since experiments have shown that this process occurs at temperatures above 600 K.^{10,34,37} In our simulations a temperature of 485 K is kept fixed in most of the simulations, even though additional simulations are performed between 470 and 490 K in order to obtain the dependence of the oscillatory period on the temperature of Figure 10. Therefore, O is removed from the surface only by reaction with CO.

(v) Oxygen atom diffusion does not occur as this process is expected to be slower compared to the remaining reaction steps, since the oxygen atoms are strongly bonded to the surface.

(vi) N diffusion is neglected since in our reaction scheme N_2 is produced preferentially through the formation of an $(\text{N}-\text{NO})^*$ intermediate and since both NO desorption and diffusion are allowed. Hence, N and NO species can easily meet at two nn cells (in contrast, in the classical reaction scheme where N_2 only is formed through the recombination of two adsorbed N atoms, N diffusion is strictly required^{8,11}). On the other hand, N

diffusion would be contrary to the experimental evidence about the formation of N-islands.

Our simulation procedure is based on the hexagonal-square (HS) model, which was originally proposed by Gelten et al. for the oxidation of CO by O_2 on a Pt(100) surface.³⁸ We believe that this method is suitable for our present study given that NO reduction by CO is similar to CO oxidation, the only differences being that in the former reaction we have more adsorbed species and that NO adsorption needs only one vacant cell, dissociation occurring in a later step, while O_2 adsorption and dissociation occurs simultaneously needing two nn vacant cells. This important difference in the particles–vacancies stoichiometry leads, however, to quite different behaviors in the kinetics of the two reactions.

Accordingly, the Pt(100) surface is represented as a regular two-dimensional (2-D) grid with periodic boundary conditions. The grid consists of $L \times L$ cells; a cell indicates one Pt surface atom, the state of each cell is described by two labels: label 1 identifies the type of molecule or atom that is adsorbed on that cell, it can also represent an empty cell, while label 2 corresponds to the presence of either the hexagonal (H) or the square (S) phases in that cell. In the square phase, each cell has four neighbors and in the hexagonal phase each cell has six neighbors. There are different (label1:label2) combinations to indicate the condition of each cell and therefore the processes that can occur on it, for instance: (H:H) indicates an empty cell in the hex phase; (X:H) an X species ($X = \text{NO}, \text{CO}, \text{N}, \text{O}$) adsorbed on a cell in the hex phase; (S:S) an empty cell in the 1×1 phase; (X:S) an X species adsorbed on a cell in the 1×1 phase. Other details concerning the HS model can be found in refs 38 and 39.

In our model, the time evolution of the system is assumed to occur as a markovian stochastic process. Under such a scheme, every elementary reaction step has a rate constant associated with the probability per unit time for the occurrence of such a step. A master equation describes the time evolution of the probability distribution of the states of the physical systems^{40,41}

$$\frac{\partial P_{\alpha}(t)}{\partial t} = \sum_{\beta} [W_{\beta \rightarrow \alpha} P_{\beta}(t) - W_{\alpha \rightarrow \beta} P_{\alpha}(t)] \quad (14)$$

Here $P_{\alpha}(t)$ is the probability to find the system in a given configuration α at time t and can be considered as a component of a vector \mathbf{P} representing the probability distribution of the whole set of system configurations, and W is the transition probability per unit time of the different processes, which are indicated as subscripts.

This master equation can be solved analytically⁴¹ only in very simple situations. In the case of the reaction considered here, it must be solved through a dynamic Monte Carlo simulation in order to avoid mean field approximations. The simulation can be performed through the “random selection method”,^{38,39} which, as adapted to our system, is as follows: (i) a surface cell is selected at random with probability $1/N$, where N indicates the total number of cells existing at the moment; (ii) a given i -type reaction step (i.e., adsorption, desorption, diffusion, etc.) is chosen at random with probability W_i/R , where R is the sum of the rates of all possible processes, i.e., the total-transition rate constant of the system; (iii) if the selected i -type reaction step is viable (according to certain rules to be specified below) on the chosen cell, then it is immediately executed, and (iv) after a given cell is selected, the time is increased by Δt according to

$$\Delta t = -\frac{\ln \xi}{NR} \quad (15)$$

where ξ is a random number selected according to a uniform probability distribution in the interval (0,1). This equation renders the real time evolution caused by a system transition.

The following elementary reaction steps and their corresponding rate constants, with the parameter values given in Table 1, are going to be considered:

Adsorption. The impinging flux of molecules of species i from the gas phase onto the surface is given by

$$J_i = \frac{p_i}{(2\pi m_i kT)^{1/2}} \quad (16)$$

where J_i is the flux of NO or CO molecules, p_i is the partial pressure of the i -type molecule, m_i is the mass of NO or CO, k is the Boltzmann constant, and T is the absolute temperature. The adsorption rate W_i of particles impinging on the surface per cell and per second is then obtained as

$$W_i = J_i A S_0 \quad (17)$$

where A is the area per cell on the surface, in this case of Pt(100), and S_0 is the initial sticking coefficient. CO and NO can be adsorbed on both the hex and the 1×1 phase.

Desorption. Desorption is considered as an activated process with a rate given by

$$W_i = \nu_i \exp(-E_{ai}/kT) \quad (18)$$

where ν_i is the frequency factor and E_{ai} the activation energy for species i .

CO and NO desorption occur both from the hexagonal and 1×1 phases at the same rate; actually, experiments indicate that these rates may be slightly different.^{6,10}

Diffusion. Diffusion jumps are allowed for both CO and NO species to vacant nn cells. These jumps can be performed on any of the two phases or across the interface between them. The diffusion rate W_i is obtained directly as a frequency factor ν_i .

NO Dissociation. On a Pt(100) surface this process can only occur on the 1×1 phase and with the availability of a vacant nn cell. According to the experimental observations of NO dissociation and to the theoretical simulations in the NO + CO reaction on Rh(111),^{9,10,22,23,31} the dissociation of NO, being a complex and the most important process, deserves separate consideration. The following features are taken into account: (a) NO dissociation is facilitated by the presence of nn coadsorbed N atoms, i.e., the dissociation probability increases with the presence of nn N, which is the mechanism we assume for the formation of N-islands;⁴² (b) the dissociation rate increases with increasing number of vacant nn cells; and (c) the blocking effect on the dissociation probability by the presence of neighboring coadsorbed NO and CO molecules. Therefore, the following expression is proposed for the dissociation rate for a NO molecule located at a given cell on the 1×1 phase

$$W_{\text{NOdis}} = \frac{W_{\text{NOdis}}(C_N n_N + C_V n_V - C_{\text{NO}}(n_{\text{NO}} + n_{\text{CO}}))}{4} \quad (19)$$

Here W_{NOdis} is an "initial" dissociation rate calculated as an activated process, as in eq 18, with appropriate frequency factor and activation energy given in Table 1, n_N is the number of nn

cells occupied by adsorbed N, n_V is the number of empty nn cells, n_{NO} and n_{CO} are the number of nn coadsorbed NO and CO species, respectively, and the coefficients C are the corresponding weighting factors.

N₂ Production. This reaction step can follow two alternative pathways: (a) through the formation of an intermediate (N–NO)* species when two nn cells are occupied by N and NO species, with a probability 0.7 multiplying the general reaction rate determined by the frequency factor and activation energy given in Table 1; (b) through the recombination of two nn adsorbed N atoms, with a corresponding probability of 0.3. The latter is completely restricted to the 1×1 phase, given that dissociated N can only exist on this phase, while the former can also take place across phase boundaries when a NO molecule is on the hexagonal phase and an N atom is on the square phase.

CO₂ Production. This process is possible when two nn cells are occupied by CO and O species. It is considered as an activated process and can take place either on the square phase or across phase boundaries when adsorbed CO happens to be on the hexagonal phase.

Surface Reconstruction. Experimental results indicate that the hex $\rightarrow 1 \times 1$ phase transition occurs by nucleation and trapping of the CO molecules and by nucleation and anisotropic growth of the NO molecules on the Pt(100) surface. This transformation of the surface is caused by the different heats of adsorption of these two species on both phases,^{33,35,43–45} which is considerably higher on the unreconstructed 1×1 phase than on the reconstructed hexagonal one.³⁶ The observations show that four to five molecules of CO are involved in the restructuring process.⁴⁶ Thiel et al. proposed for CO molecules that this transformation occurs by a sequential mechanism: initially, the 1×1 phase is formed by nucleation of adsorbed CO molecules on a precursor hexagonal phase, followed by the migration and trapping of the CO molecules by way of growing islands.⁴⁵ On the other hand Mase et al. reported that the hex $\rightarrow 1 \times 1$ transition phase takes place by nucleation and by growing islands of adsorbed NO molecules.³⁵ These similar processes that occur in the phase transition driven by adsorption of CO and NO can be understood by considering the experimental evidence that the heats of adsorption of both molecules are almost the same.³⁶

Incorporating these experimental results into our model, we assume the following two mechanisms: (i) the *nucleation* mechanism for the hex $\rightarrow 1 \times 1$ reconstruction takes place if there exist five adsorbed molecules (CO, NO, or a mixture of both) forming a nucleating cluster; (ii) CO, NO, and CO/NO-island growth on the square phase happens through a *trapping* mechanism, i.e., when a molecule on the hexagonal phase is in a nn position to a molecule belonging to a reconstructed 1×1 island, then it is trapped into that island and its cell reconstructs from the hexagonal to the square phase. The rates for these two processes are determined directly by appropriate frequency factors.

Considering that the 1×1 geometry is metastable compared to the hex geometry, we have taken into account that the inverse $1 \times 1 \rightarrow$ hex transformation occurs in empty cells of the square phase. In this analysis, a single empty cell can perform this transformation, which is considered as an activated process with appropriate frequency factor and activation energy.^{6,10,43}

These similar behaviors between CO and NO induced hex $\rightleftharpoons 1 \times 1$ surface phase transition have been demonstrated experimentally.^{6,10}

TABLE 1: Values of the Parameters Used in Simulations and Their Comparison with Their Experimentally Observed Values

reaction	p^{exp} (Pa)	p^{sim} (Pa)	S_0^{exp}	S_0^{sim}	ref
CO adsorption	4.0×10^{-4}	3.9×10^{-4}	≈ 0.8	0.8	4, 36, 46
NO adsorption	4.0×10^{-4}	4.0×10^{-4}	≈ 0.8	0.8	4, 36
CO desorption	4×10^{12} to 1×10^{15}	1×10^{11} to 1×10^{15}	115–157	147–158	6, 10
NO desorption	1.7×10^{14} to 10^{15}	1×10^{11} to 1×10^{15}	142–155	147–158	6, 10
NO dissociation	1×10^{15} to 2×10^{16}	1×10^{15}	117–134	126–133	6, 10
N ₂ production	1.3×10^{11}	1×10^{11}	84.6	90	10
CO ₂ production	2×10^8 to 10^{10}	2×10^{10}	50–100	83.5	6, 10, 38
$1 \times 1 \rightarrow \text{hex}$	2.5×10^{10} to 10^{11}	3×10^{10} to 1×10^{11}	103–107	105–106.5	6, 10, 43
CO/NO nucleation		0.015–0.03	≈ 0	0	25, 35, 43–45
CO/NO trapping		0.015–0.03	≈ 0	0	25, 34–36
CO diffusion		0–100			24, 25, 38
NO diffusion		0–100			24, 25

3. Results and Discussion

In our simulations the partial pressures of reactants in the gas phase are kept constant. Experiments show that NO reduction by CO on Pt(100) displays irregular, chaotic, and sustained oscillations on a local scale, and damped oscillations on a global scale in the temperature range of 470–490 K and partial pressures of NO and CO of about 10^{-4} Pa.⁴ However, it should be kept in mind that the length scales for experiments and simulations are very different, the former being several orders of magnitude larger than the latter, therefore what is considered as a local scale in experiments could correspond to a global scale in simulations. The partial pressures of NO and CO for our analysis were chosen as 4×10^{-4} Pa and 3.87×10^{-4} Pa, respectively. Unless explicitly mentioned (as in section 3.4) the values of the weighting factors used in the eq 19 will be kept fixed at $C_N = 0.7$, $C_V = 0.7$, and $C_{NO} = 0.2$, values obtained by adaptation of those used in ref 23 to the case of a square lattice.

The principal results of the CO + NO reaction simulation study will be now presented. Afterward, a discussion concerning the effect that each reaction step or surface process can produce on the behavior of the system will be undertaken. For the sake of simplicity, some of the reaction parameters will not be specifically mentioned throughout this discussion, since these quantities are thought to have little influence on the development of the different kinetic oscillation types and on the formation of assorted surface patterns. Table 1 shows the values of the parameters that have been employed in our simulations in order to obtain the rate of each elementary reaction step; experimental values of these parameters are also included for comparison. Since no available data account for the decay of the (N–NO)* complex intermediate to N₂ and consequently for the value of the corresponding rate constant, we have instead employed for this assignment the experimental values of N₂ formation proceeding from the classical N + N recombination. As already mentioned, the fact that the (N–NO)* pathway is faster than the N + N pathway is taken into account by an additional probability factor of 0.7 for the first and 0.3 for the second.

3.1. Synchronization Mechanism. According to the experimental data on the reduction of NO by CO on Pt(100), sustained rate oscillations can occur at elevated temperatures ($T > 478$ K). Under such circumstances, the oscillations are due to the hex $\rightleftharpoons 1 \times 1$ phase transition; the appearance of these temporal patterns has been explained through the formation of a synchronized phase transition mechanism.^{3,4} Nevertheless, at lower temperatures the oscillatory behavior can be observed on a local scale on a homogeneous 1×1 substrate without the involvement of the hex $\rightleftharpoons 1 \times 1$ phase reconstruction, in this case there is no synchronized mechanism and no sustained rate oscillations exist.⁴ In our study, corresponding to the higher

temperature region, the appearance of sustained oscillations is possible by means of the development of a synchronized hex $\rightleftharpoons 1 \times 1$ phase transition mechanism. Moreover, sustained oscillations are usually associated to the formation of cellular structures. This synchronized mechanism can be explained as follows.

The simulation of the NO + CO reaction on the Pt(100) surface starts from a completely hex-reconstructed clean surface, on which it is feasible to observe the adsorption of both CO and NO molecules. At a certain surface coverage, small nuclei of CO, NO, or CO/NO mixtures form on the surface according to certain probability values; these clusters can then transform small surface regions from the hex to the square phase thus forming 1×1 CO, 1×1 NO, and 1×1 CO/NO islands. Afterward, these nuclei can grow by trapping reactions; this part of the evolution of the system is known as the *transformation stage*. The growth of these islands is a stable process, since the reaction can be locally inhibited by a relatively high adsorbate coverage, which prevents the dissociation of NO. However, when either a CO or NO molecule desorbs from the square phase surface toward the gas phase, or if a CO or NO molecule diffuses from the square phase toward the hexagonal phase (the diffusion processes can occur across the interface), an empty cell appears and, if this vacancy has a nn adsorbed NO molecule, then this NO molecule has the possibility of dissociating into N and O atoms. Now, it is pertinent to recall that the 1×1 phase is the one that is active for NO dissociation, while the hex phase is not. If this dissociation step is accomplished, the adsorbed oxygen atom can then react with an adsorbed CO molecule while, in turn, the adsorbed N atom can also react either with an adsorbed NO molecule, thus forming the (N–NO)* complex intermediate, or with another N adsorbed atom. The species that are formed on the surface can desorb as CO₂ and N₂ into the gas phase. Thus, new vacant cells can form on the 1×1 phase allowing more NO adsorbed molecules to dissociate; subsequently, more O and N atoms can continue reacting, leading to an autocatalytic “explosive” surface reaction. In this way, a reaction front starts to propagate across the surface. As a result of this process, a *reactive stage* is developed on the 1×1 phase. As vacant cells existing on the square phase have a finite probability of undergoing the $1 \times 1 \rightarrow \text{hex}$ reconstruction, then small areas of the surface can slowly return to the hexagonal configuration. This last process is known as the *recovery stage*, in this way the reactive stage is gradually extinguished. CO, NO, and CO/NO nuclei will be formed once more, and the oscillatory cycle will resume again from the transformation stage.

While Gelten et al. proposed a similar synchronized mechanism in their simulation model related to CO oxidation on Pt(100),³⁸ this kind of oscillatory cycle was observed experimentally for the NO + CO reaction on Pt(100) surfaces, showing

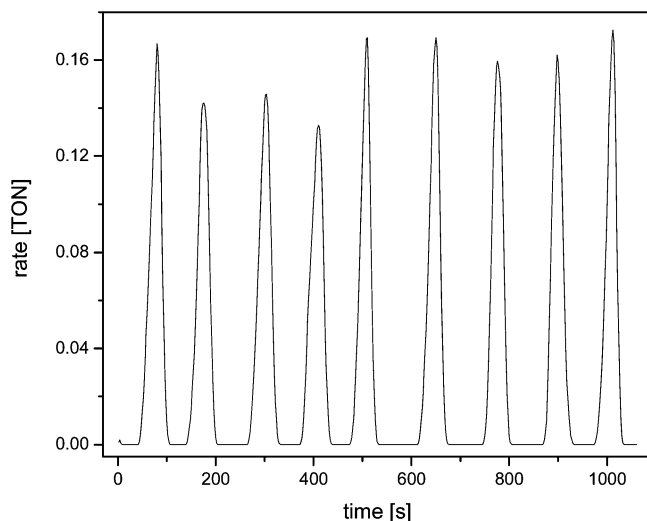


Figure 1. Sustained oscillations: CO_2 production rate in turnover number (TON). Rates for $W_{\text{COdes}} = W_{\text{NOdes}} \approx 1 \times 10^{-6} \text{ s}^{-1}$; $W_{\text{COdif}} = W_{\text{NOdif}} = 50 \text{ s}^{-1}$; $W_{\text{H}\rightarrow\text{S}} = 0.015 \text{ s}^{-1}$; $W_{\text{S}\rightarrow\text{H}} \approx 0.1 \text{ s}^{-1}$; $W_{\text{NOdis}} \approx 15 \text{ s}^{-1}$.

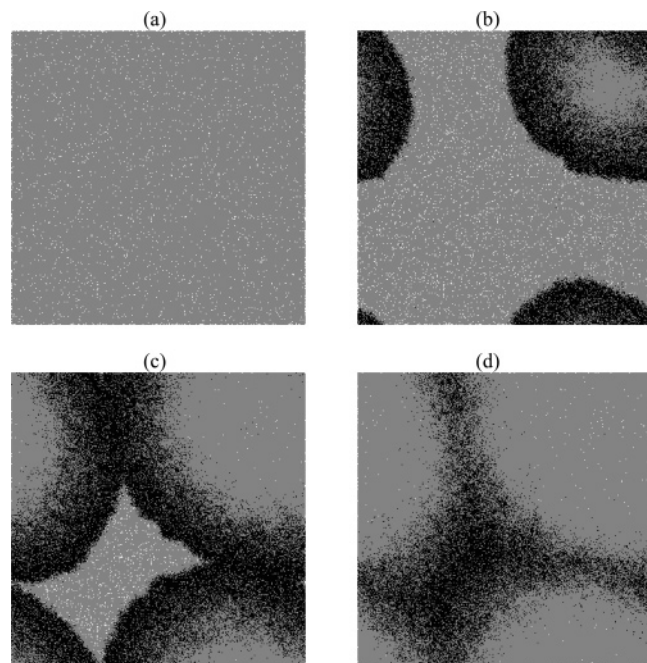


Figure 2. Snapshots corresponding to oscillations of Figure 1. Gray areas indicate CO/NO on the hexagonal phase, white areas show CO/NO on the 1×1 phase, and black areas are N, O, and empty cells on the hexagonal and 1×1 phases.

the role of defects on the surface, which facilitate NO dissociation on the 1×1 phase.⁴

The above scenario is depicted in Figures 1 and 2. In Figure 1, we can observe sustained oscillations obtained from a simulation performed on a lattice with 1024×1024 cells at $T = 485 \text{ K}$. In such a figure, it is possible to visualize the rate of production of CO_2 measured as turn over number (TON), i.e., the number of CO_2 molecules produced per Pt atom per second. Figure 2 shows the formation of a cellular pattern, i.e., snapshots of the surface evidencing the existence of the synchronized mechanism: Figure 2a depicts the *transformation stage* at 40 s. Figure 2b represents the *reactive stage* at 65 s. Here we can clearly see the formation and growing of a reaction front spreading across the surface. This reaction front is not inhibited by the boundaries. Figure 2c shows that when this front grows sufficiently in size, it collides with itself and starts to extinguish

at a time of 80 s. Figure 2d shows how the reaction front is extinguished almost totally after 90 s have passed. here we can observed that the *recovery stage* is in progress.

Analogous reaction fronts and their subsequent propagation were also reported by Tammaro and Evans for the $\text{NO} + \text{CO}$ reaction on a Pt(100) surface via the standard mean-field reaction–diffusion equations.¹³ Experimentally these cellular patterns have been observed for the $\text{CO} + \text{O}_2$ reaction taking place on a Pt(110) surface.⁴⁷

3.2. Influence of CO and NO Diffusion. We have found in this work that CO and NO surface diffusion processes are very important in the behavior of the system. In fact, diffusion is the principal means to achieve the synchronization mechanism in simulations. For this reason, its influence will depend on the grid size used in simulations. By change in the rates of these diffusion processes different oscillatory behaviors are observed according to the following characteristics:

(a) When both CO and NO diffusion rates are relatively low, equal to 10 s^{-1} , and if the grid size is 64×64 cells or less, sustained oscillations can be observed. But, if the grid size increases, the sustained oscillations decay into irregular oscillations. This result is due to the fact that, on intermediate or large grids (128×128 cells or more) with slow mobility of the molecules, too many reaction fronts are created on the surface and collide with others, although these fronts do not lead to complete extinction. Remnants of these reaction fronts can still survive when new fronts are generated on the surface; the recovery stage is no longer observed thus destroying the synchronized oscillatory behavior. Sustained oscillations appear on relatively small grid sizes due to the creation of fewer reaction fronts on the surface.

When the rates of CO and NO diffusion are increased, for example to 50 s^{-1} , on medium or large grids, the irregular oscillations are transformed into sustained oscillations. This can be explained by the relatively high CO and NO diffusion rates, which induce CO and NO molecules to move faster on both surface phases, and as the diffusion processes by both molecules are not hindered by phases boundary, few reaction fronts are created on the surface; these fronts collide and are extinguished (see Figure 2), the recovery stage is obtained, and therefore the synchronized oscillatory behavior can be observed on the surface.

If the rates of both diffusion processes are increased even more, the periods of the sustained oscillation become longer, because the reaction between the adsorbed species is delayed due to the high mobility of CO and NO. This same behavior is observed when the CO diffusion rate is larger than that of NO, because the empty cells of the 1×1 phase are preferentially occupied by CO. In this way NO dissociation is delayed and therefore the reaction among the species is obstructed. Similar effects were also observed in other simulations performed on a Pt(100) surface, both for the $\text{NO} + \text{CO}$ reaction and for the $\text{CO} + \text{O}_2$ reaction.^{15,24,38}

(b) When the NO diffusion rate is larger than that of CO, the original sustained oscillations transform into irregular or modulated ones. Irregular oscillations occur in view of the fact that, if NO molecules can move faster than CO molecules, when NO dissociation occurs CO molecules are no longer capable of consuming all O atoms and a small amount of oxygen remains on the 1×1 phase. Modulated oscillations will be discussed below in section 3.4.

(c) When CO diffusion is taken into account, while NO diffusion is neglected, oscillations are not obtained. This is due to the fact that, since CO diffusion is not hindered by phases

boundaries, the vacant cells of the 1×1 phase are then occupied by CO and the square phase becomes saturated by CO; therefore NO dissociation does not occur and the amount of oxygen on the surface is not enough to consume the adsorbed CO.

(d) If the NO diffusion rates have suitable values and CO diffusion is neglected, oscillations are not observed in the system, since CO molecules do not have mobility on the surface and cannot consume all adsorbed O atoms; therefore small O-islands are formed, which grow and slowly poison the surface.

In a previous study²⁵ we have found that CO diffusion was more important than NO diffusion, since sustained oscillations were obtained when NO diffusion was neglected, while oscillations were not observed when CO diffusion was suppressed. This difference is due to the fact that, in that work, the diffusion processes of both molecules were allowed on any of two phases but not across the interface between them. In the present work, where we consider CO and NO diffusion on the two phases and across the phase boundary, both CO and NO diffusion have the same importance since, if any of these processes are not taken into account in the system, oscillations are not observed. This result is more consistent with the experimental evidence: both CO and NO molecules are mobile adsorbates, the diffusion of both species can spread the reaction and ignite spatially adjacent regions through the formation of reaction fronts, originating spatiotemporal pattern and oscillations.¹

3.3. Effects of NO and CO Desorption. As it can easily be seen, CO and NO desorption processes are the most important promoters for the formation of reaction fronts. If these desorption processes are neglected, the oscillatory behavior can never be produced and the 1×1 phase will eventually become poisoned by CO and NO molecules. As a consequence, either CO or NO desorption would trigger oscillations. In our simulations, regular sustained oscillations are obtained if the rate constants for desorption processes have values between 1×10^{-4} and $1 \times 10^{-2} \text{ s}^{-1}$ in medium and large size grids. If these rates are slower, the size of the sustained oscillation period is not constant. As the CO and NO partial pressures are almost the same, the rates of adsorption are expected to be similar for both gases. For these reasons, CO and NO desorption rates are estimated to be about equal for both molecules. If the desorption rate constants of CO and NO are increased and the diffusion rate constants for CO and NO molecules have the same high value (50 s^{-1}), the oscillation period becomes shorter. If these desorption rates are increased even more, the sustained oscillations will begin to decay into irregular ones. If the diffusion rates decrease (10 s^{-1}), then sustained oscillations are transformed into damped oscillations. This kind of behavior can be understood by considering that desorption and reaction processes compete with each other: if CO and NO desorption rates are too high, then these two species are eliminated from the surface faster than through the reactions producing CO_2 and N_2 . Moreover, by slowing the mobility of CO and NO molecules, the surface in the global scale presents an inhomogeneous behavior. This fact had already been observed in previous studies.^{24,25} Figure 3 shows damped oscillations obtained on a lattice with 1024×1024 cells at $T = 485 \text{ K}$.

3.4. NO Dissociation Effects. The most regular and sustainable oscillatory patterns are obtained when the initial NO dissociation rate constant (W_{NOdis}) has a value of about 15 s^{-1} and the values of the weight factors used in eq 19 are $C_{\text{N}} = 0.7$, $C_{\text{V}} = 0.7$, and $C_{\text{NO}} = 0.2$. When the values of the initial NO dissociation rate and of the weight factors are changed, the following behaviors are observed:

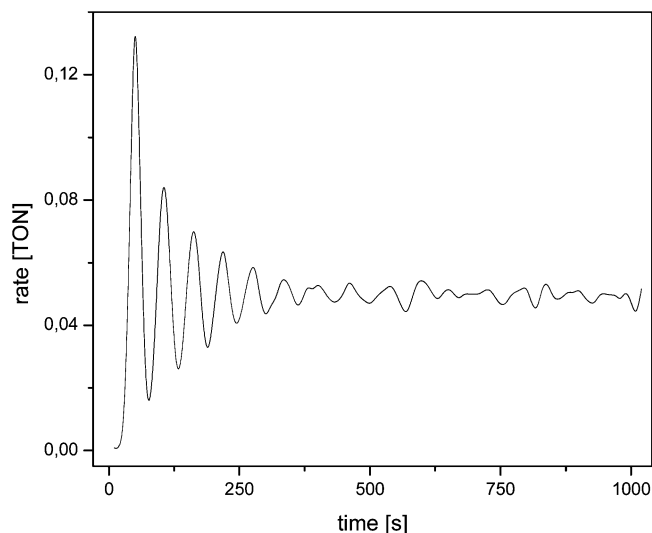


Figure 3. Damped oscillations: CO_2 production rate in turnover number (TON). Rates for $W_{\text{COdes}} = W_{\text{NOdes}} \approx 1 \times 10^{-4} \text{ s}^{-1}$; $W_{\text{COdif}} = W_{\text{NOdif}} = 10 \text{ s}^{-1}$; $W_{\text{H-S}} = 0.015 \text{ s}^{-1}$; $W_{\text{S-H}} \approx 0.1 \text{ s}^{-1}$; $W_{\text{NOdis}} \approx 15 \text{ s}^{-1}$.

(a) When the initial rate is increased, the oscillation period becomes shorter. This happens because there are many O and N atoms on the surface and, if the adsorbed CO or NO molecules have high diffusion rates (50 s^{-1}), these atoms can then react rapidly to produce CO_2 and N_2 . If the NO dissociation rate increases even more, the sustained oscillations decay into a modulated behavior. This interesting phenomenon is obtained when the initial NO dissociation value is increased by a factor of about 2. This behavior is shown in Figure 4, where, in addition to the CO_2 production rate (a), also the N_2 production rate (b) is included. Here N_2^* means N_2 production via the $(\text{N}-\text{NO})^*$ intermediate complex, N_2^{RS} means N_2 production via the $\text{N} + \text{N}$ recombination step, and N_2 means N_2^* plus N_2^{RS} , that is, the N_2 total production. Our experience indicates that the manifestation of this oscillatory behavior could be due to a competing effect between the NO dissociation rate and the N_2 production rate.²⁴ In fact, when the initial NO dissociation rate is smaller than the N_2 production rate, sustained oscillations are observed; when the initial NO dissociation rate is equal to the N_2 production rate, the sustained behavior decays into an irregular one; if the initial NO dissociation rate is further increased gradually, the irregular behavior is transformed in a pulsed oscillation. It is usually believed that this kind of phenomenon is to be expected when an additional feedback loop is added to the reaction scheme.⁴⁸ This could be true in our case, since we have included a parallel reaction in the N_2 production into the classical reaction mechanism, namely, the $(\text{N}-\text{NO})^*$ pathway. However, by looking at Figure 4b, we see that the contribution of N_2^{RS} to N_2 production is much smaller than that due to N_2^* : the contribution of N_2^{RS} is between 1.5% and 3% of the total N_2 . Even more, if the $\text{N} + \text{N}$ recombination pathway is suppressed, that is $\text{N}_2^{\text{RS}} = 0$, the above behavior is maintained (this effect will be discussed with detail in section 3.5). Therefore, in our study the additional feedback loop in the reaction mechanism is not responsible for the observation of modulated oscillations.

In section 3.2(b) we observed that when the NO diffusion rate is larger than that of CO, sustained oscillations decay into modulated ones. We now attempt an explanation for this: As NO molecules have more mobility on the surface, they have more opportunity to find appropriate cells with vacant nm, thus producing a bigger effective NO dissociation rate; this, as discussed above, would produce modulated oscillations.

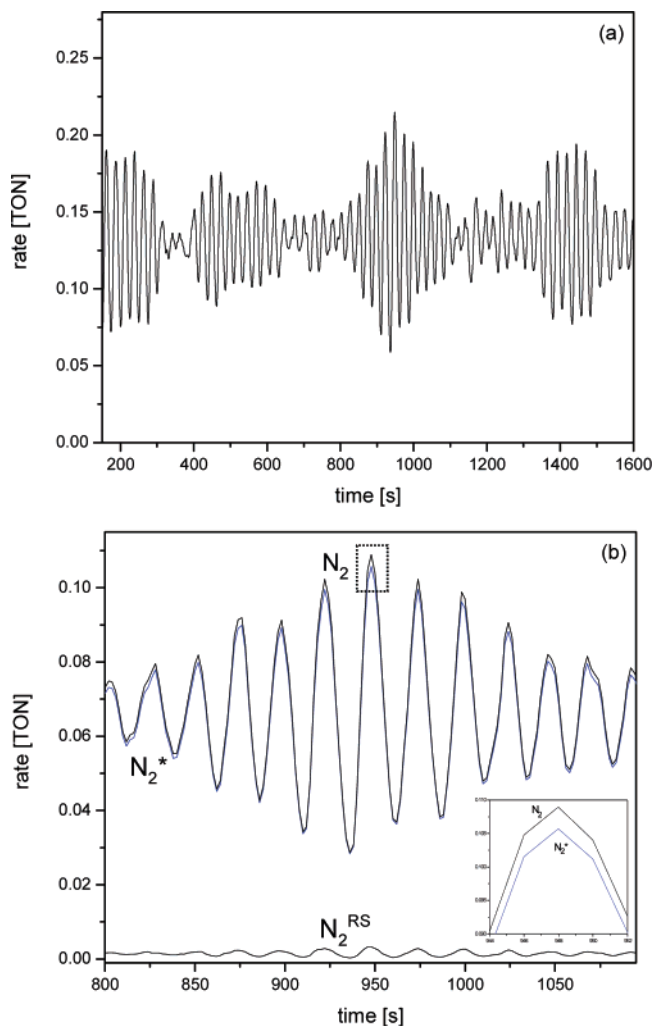


Figure 4. Modulated oscillations at $T = 485$ K: CO_2 (a) and N_2 (b) production rate in turnover number (TON). Rates for $W_{\text{COdes}} = W_{\text{NOdes}} \approx 1 \times 10^{-6} \text{ s}^{-1}$; $W_{\text{COdif}} = W_{\text{NOdif}} = 50 \text{ s}^{-1}$; $W_{\text{H-s}} = 0.015 \text{ s}^{-1}$; $W_{\text{s-H}} \approx 0.1 \text{ s}^{-1}$; $W_{\text{NOdis}} \approx 30 \text{ s}^{-1}$. Grid size: 512×512 cells.

(b) When the initial rate is decreased, the contrary behavior is observed, that is, the oscillation period becomes longer, because with a low NO dissociation rate there are few adsorbed O and N atoms and therefore the adsorbed CO and NO species react slowly. But, if the initial NO dissociation rate constant decreases by a factor of more than 5, the oscillations end, since the amounts of O and N are not enough to sustain the oscillatory behavior.

(c) According to eq 19, the NO dissociation rate is modified by the factors with weights C_N , C_V , and C_{NO} , representing the effects of N-islands, of enhancement due to vacant nn sites and of depression due to coadsorbed nn NO or CO, respectively. We shall now study what happens when each of these effects is “turned off”. First, we consider the suppression of the effect of N-island formation, by making $C_N = 0$. In this case, the NO dissociation probability is not enhanced by the presence of coadsorbed nn N atoms; therefore the rate is on average lower and, as already discussed above, the oscillation period becomes longer. However, as it can be observed in Figure 5, the effect is very small indicating that only small N-islands are formed on the surface (as it can also be seen in simulation snapshots, not shown here). A similar behavior of the oscillation period is observed by making $C_V = 0$.

(d) Next, we analyze the effect of depressing the NO dissociation rate due to coadsorbed nn CO and NO molecules.

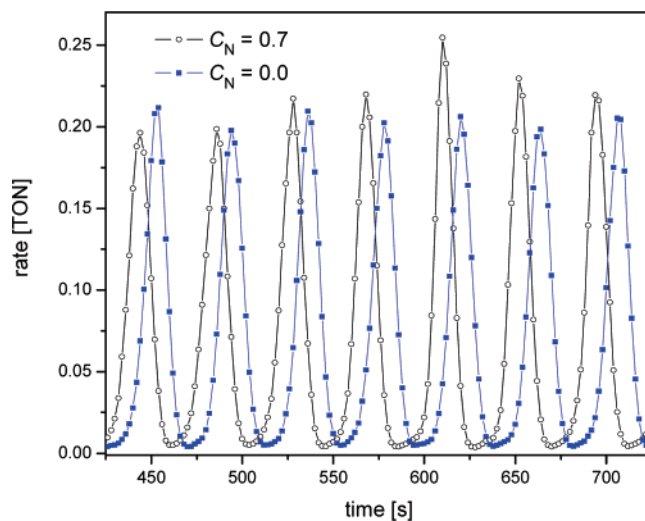


Figure 5. Effect of neglecting the process in the N-island formation during the oscillatory behavior at $T = 485$ K. Rates for $W_{\text{COdes}} = W_{\text{NOdes}} \approx 1 \times 10^{-2} \text{ s}^{-1}$; $W_{\text{COdif}} = W_{\text{NOdif}} = 50 \text{ s}^{-1}$; $W_{\text{H-s}} = 0.015 \text{ s}^{-1}$; $W_{\text{s-H}} \approx 0.1 \text{ s}^{-1}$; $W_{\text{NOdis}} \approx 15 \text{ s}^{-1}$. Grid size: 512×512 cells.

When we suppress this effect by setting $C_{\text{NO}} = 0$, the following results are found: (i) if $W_{\text{NOdis}} \approx 15 \text{ s}^{-1}$, oscillations are not obtained; (ii) if $W_{\text{NOdis}} \approx 3 \text{ s}^{-1}$, only damped oscillations are observed; (iii) if the initial NO dissociation rate is decreased even more, the oscillations disappear, since, as was explained above, whenever the initial NO dissociation rate is reduced by a factor of more than 5, no oscillatory behavior is obtained. Now, if we take $C_{\text{NO}} = 0.1$, the following behavior is observed as compared with the case with $C_{\text{NO}} = 0.2$: (i) if $W_{\text{NOdis}} \approx 15 \text{ s}^{-1}$, the original sustained oscillations are transformed into damped oscillations; (ii) if $W_{\text{NOdis}} \approx 3 \text{ s}^{-1}$, sustained oscillations are obtained; (iii) if the initial NO dissociation rate is decreased even more, the oscillations disappear. In short, when the weight factor C_{NO} decreases, the NO dissociation rate increases rapidly, so damped oscillations are observed and therefore sustained oscillations can be obtained by decreasing the initial rate. When the weighting factor C_{NO} is neglected, only damped oscillations can be observed.

This important result shows that the inhibition effect on the dissociation of NO by coadsorbed CO and NO molecules is crucial for the system in order to obtain sustained oscillations. As already mentioned, this effect was also found crucial in steady-state studies²³ in order to achieve a concordance between the O coverage in simulations with the experimentally observed values. In addition, when the weight factor C_{NO} is taken into account, CO/NO islands are formed on the 1×1 surface phase. This fact is also in concordance with experimental observations. In fact, an important factor leading to the development of sustained oscillations in the real system is the hex $\rightarrow 1 \times 1$ phase transition, which proceeds through the growth of 1×1 -CO/NO islands in the NO + CO reaction on Pt(100) surface in the high-temperature range.^{4,6,7,10}

3.5. Effect of Alternative Pathways on N_2 Production.

Given that N_2 production is achieved through the formation of the (N-NO)* intermediate in parallel with the classical N + N recombination step, we study now the relative importance of these two pathways on the behavior of the oscillations.

First, we consider the elimination of reaction step (12); therefore N_2 production is only due to the formation and decay of the (N-NO)* activated complex. This leads to an increase in the oscillation period, but the effect is very small as shown in Figure 6 with a grid size of 512×512 cells at $T = 485$ K.

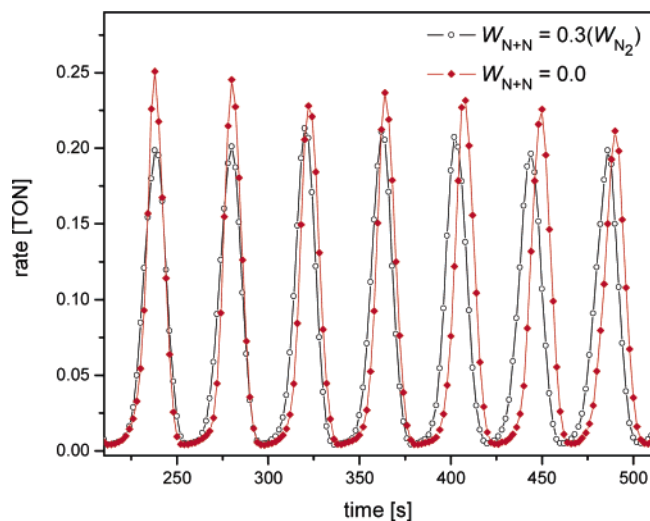


Figure 6. Effect of the suppression the $N + N$ recombination step for the formation of N_2 . The designations of the rates are as in Figure 5.

N_2 production is delayed and so is CO_2 production, due to the fact that the stoichiometry between CO_2 and N_2 is always maintained. The smallness of this effect indicates that the coverage of adsorbed N atoms is always small, so that they are not decisive for creating oscillations in the system. This fact is also in concordance with the experiments and it happens because N atoms are rapidly removed from the surface,^{6,9,10} in this case through adsorbed NO molecules by forming $(N-NO)^*$ intermediary species.

Next, we consider the suppression of reaction steps (10) and (11), assuming now that the only way to produce N_2 is through the classical $N + N$ recombination step. This leads only to the formation of damped oscillations on the surface. The amount of adsorbed N atoms increases quickly on the surface, but they react slowly, because the diffusion of N atoms is neglected in this study and a large N atom coverage remains on the surface. Produced N_2 comes mainly from the formation of small N -islands, which disappear quickly as they are consumed by the reaction, thus producing a damped oscillatory pattern. As sustained oscillations have also been observed in the real system, and this behavior can be only obtained by including the $(N-NO)^*$ pathway in the simulation, this indicates that the formation of the $(N-NO)^*$ complex and its subsequent decay to $N_2(gas)$ and adsorbed O atoms is the most important reaction step for the formation of different types of oscillations in the NO reduction of CO on a $Pt(100)$ surface. Figure 7 shows this behavior at $T = 485$ K for a grid of 512×512 cells: Figure 7a indicates the rate of production of CO_2 in turn over number (TON) and Figure 7b shows the surface coverage of each adsorbed species measured in monolayers (ML) on the square phase. In the latter figure we observe that the N atom coverage increases initially and then stays approximately constant for a long time with small oscillations indicating that N -islands on the 1×1 phase of the surface of $Pt(100)$ are being formed and consumed.

3.6. Effect of the Surface Reconstruction. The model employed here is very sensitive to the $hex \rightarrow 1 \times 1$ phase transition. If nucleation and trapping rates have frequency values of $0.015 s^{-1}$, sustained oscillations can be observed. If these values are increased, the sustained oscillations decay toward irregular oscillations. The transformation stage is faster than the recovery stage, since an empty cell that undergoes $1 \times 1 \rightarrow hex$ phase transition can be occupied by either a CO or NO molecule and quickly reconstructs toward the square phase by

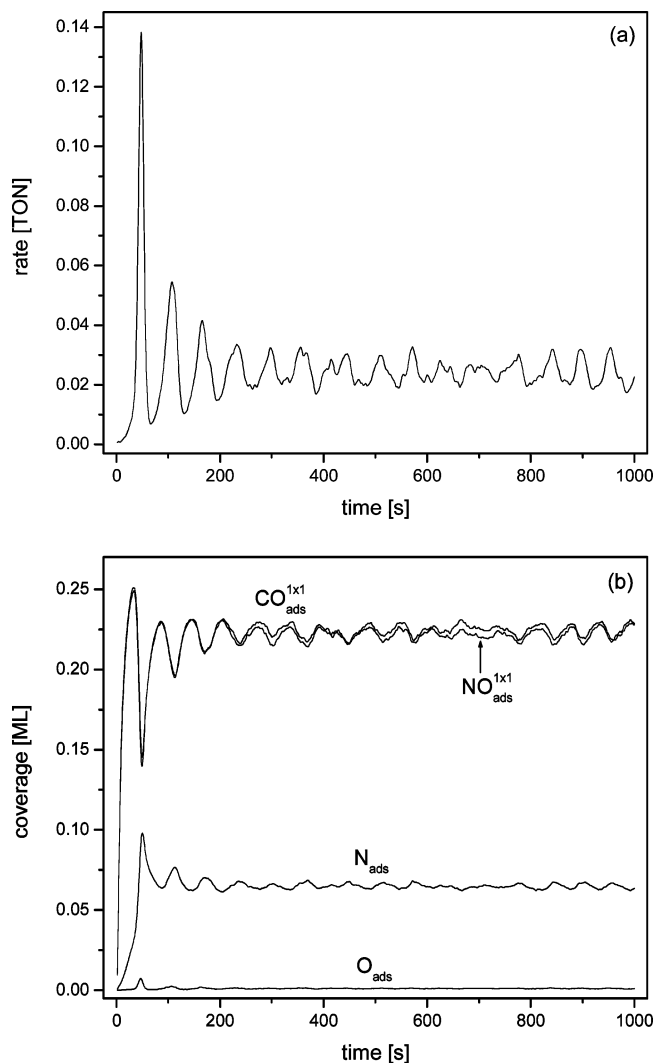


Figure 7. Effect of neglecting the $(N-NO)^*$ intermediate in the formation of N_2 : (a) CO_2 production rate in turnover number (TON); (b) coverage of adsorbed species on the square phase. The designations of the rates are as in Figure 5.

means of trapping or nucleation reactions. Such molecules can desorb from the square phase and, if NO dissociates, a new reaction front is formed, while the old reaction fronts are not completely extinguished. This destroys the synchronized mechanism. If the rate constants are decreased, the oscillation periods are longer, the nucleation and the trapping reactions are slower, and the transformation stage is deferred.

On the other hand, when the $1 \times 1 \rightarrow hex$ transformation rate attains a value of about $0.1 s^{-1}$, sustained oscillations are observed. If this transformation rate is decreased, the sustained pattern declines in favor of an irregular behavior; the square phase cannot reconstruct into the hexagonal phase, i.e., the recovery stage has not enough strength for this to be completed, then destroying the synchronized mechanism. Nevertheless, if this same rate is increased, the oscillation period becomes shorter, and if such a rate is increased even more, irregular oscillations are observed.

3.7. Effect of the Grid Size. We have found that when a sustained oscillatory behavior declines in favor of irregular, damped, or modulated regimes, then the cellular patterns decay into turbulent spatial patterns. The clearest signals of spatiotemporal behaviors are obtained when using large grids, i.e., 512×512 cells or larger. Figure 8 shows the cellular structures and their successive decline into turbulent regimes, these

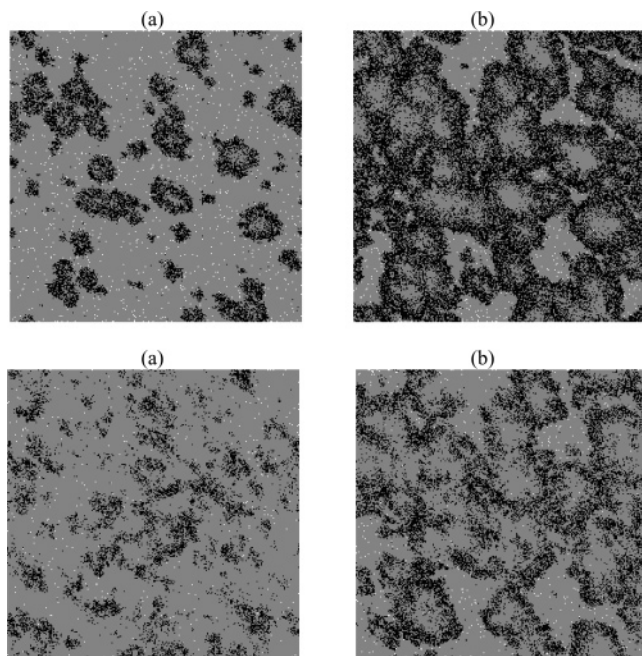


Figure 8. Pattern formation during a simulation on a grid of 1024×1024 cells: (a) cellular patterns formation at 35 s; (b) growth of the cellules and collision between them at 45 s; (c) turbulent pattern formation at 100 s; (d) the turbulent behavior is preserved at 300 s. The color of the areas is the same as those in Figure 2.

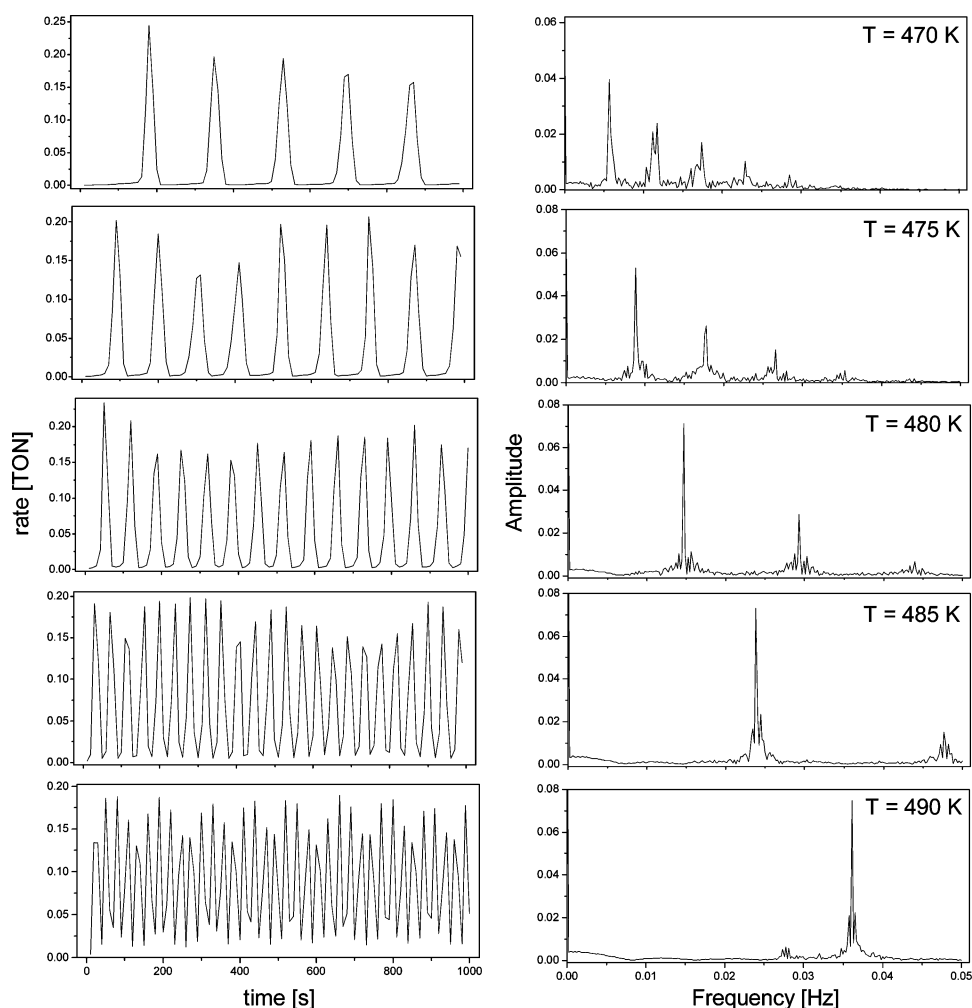


Figure 9. Oscillations with corresponding power spectra at different temperatures. Each power spectrum was calculated over a simulation run during 5000 s. The oscillations are shown only over 1000 s. Rate constants: $W_{\text{COdif}} = W_{\text{NOdif}} = 50 \text{ s}^{-1}$; $W_{\text{H-s}} = 0.015 \text{ s}^{-1}$. Grid size: 512×512 cells.

snapshots correspond to the damped oscillations of Figure 3. Turbulent patterns have been observed both experimentally and theoretically in the $\text{NO} + \text{CO}$ reaction on the $\text{Pt}(100)$ surface.^{1,4,15} It is pertinent to mention that on small grids (32×32 and 64×64 cells) oscillations are not very well defined, while on intermediate grid sizes (i.e., 128×128 and 256×256 cells) oscillations are already observed. In a grid of 256×256 cells, a reaction front can be readily created. This front can then collide with others and can be extinguished throughout boundary periodic conditions. Also, it is worth mentioning that in large grids good quality sustained oscillations can be produced if the values of the rates of CO and NO diffusion are high as explained in section 3.2.

3.8. Influence of Temperature. Finally, we have studied the effect of the temperature in the system. In our simulations we have observed that if the temperature increases, the oscillation period decreases. This result is in concordance with the experimental observations on the NO reduction by CO on a $\text{Pt}(100)$ surface: (i) Vesper and Imbihl observed that the oscillation frequency increases when the temperature increases in the range between 470 and 490 K.⁴ (ii) Fink et al. found that oscillation period decreases when the temperature increases in the system; however, it is important to mention that this experiment was performed at $T < 470 \text{ K}$ and that only damped oscillations were obtained.⁶

We believe that this behavior appears in the $\text{NO} + \text{CO}$ reaction on the $\text{Pt}(100)$ surface, because when the temperature

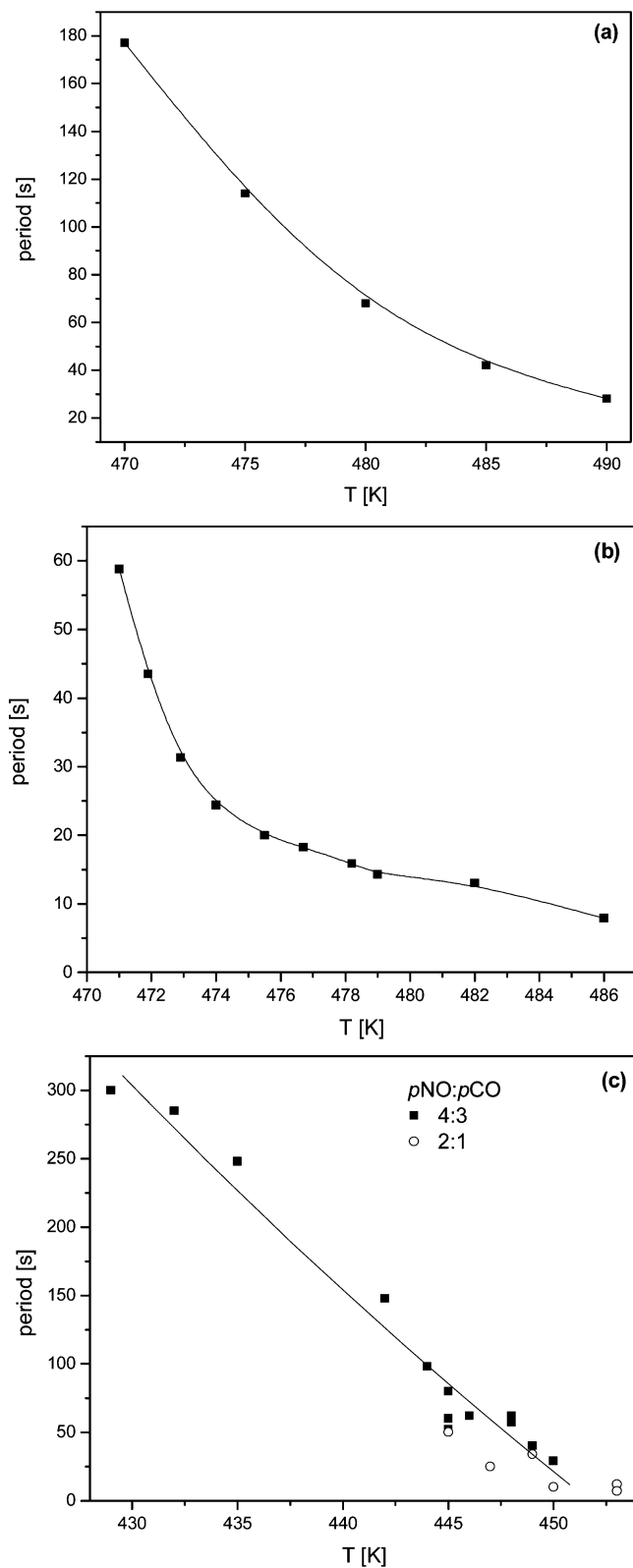


Figure 10. Dependence of oscillation period on the temperature. (a) Simulation results. Rate constants: $W_{CO_{diff}} = W_{NO_{diff}} = 50 \text{ s}^{-1}$; $W_{H-S} = 0.015 \text{ s}^{-1}$. Grid size: 512×512 cells. (b) Experimental results extracted from refs 3 and 4 for $p_{CO} = p_{NO} = 4 \times 10^{-4} \text{ Pa}$. (c) Experimental results extracted from ref 6 for $p_{NO}:p_{CO} = 4:3$, with a total pressure of $7 \times 10^{-5} \text{ Pa}$, and for $p_{NO}:p_{CO} = 2:1$, with a total pressure of $9 \times 10^{-5} \text{ Pa}$.

is increased the adsorption rates of CO and NO decrease very little, with a negligible effect on the behavior of the system, since these rates depend strongly on the gas pressures, while

the other rates increase drastically, except for the diffusion and $\text{hex} \rightarrow 1 \times 1$ phase transition rates, which are not considered here to depend on the temperature. Therefore, the system behavior is more dynamic, that is, as CO and NO desorption and NO dissociation rates increase, oscillation periods are shorter (see sections 3.3 and 3.4). Figure 9 shows the changes in the oscillations and their spectral frequencies as the temperature rises. It can be seen that the frequency increases notably; as a result the oscillation period decreases.

Figure 10 shows the dependence of the oscillation periods with the temperature observed in our simulations (a) and in experiments (b) and (c). Simulation results are between the two sets of experimental data. As it can be seen, experimental data depend strongly on the pressure in the gas phase. This is so because in experiments the synchronization mechanism generating the oscillations is mainly achieved via global coupling through the gas phase. On the contrary, in simulations this is achieved via the diffusion of adsorbed species, which does not depend on the pressure in the gas phase. Under these considerations, the observed qualitative agreement between simulations and experiments turns out to be satisfactory.

4. Conclusions

We have studied by dynamic Monte Carlo simulations the oscillatory behavior of the NO + CO reaction on Pt(100) in the high-temperature range and low pressures under the hypothesis that the main reaction step leading to the formation of N_2 is not only through of the classical $\text{N} + \text{N}$ recombination step but, and principally, through the formation of the $(\text{N}-\text{NO})^*$ intermediate, as suggested by experiments performed on Rh(111). In addition, other relevant experimental observations have been included in the present study regarding the NO dissociation rate, which is enhanced by the presence of coadsorbed nn N atoms (effect of N-islands formation) and by the presence of nn vacant cells, while it is depressed by the presence of coadsorbed nn NO and CO molecules.

The principal result of the present study is the appearance of a sustained oscillatory behavior associated with the formation of bubble-like patterns, in contrast to the behavior found when only the classical mechanism is taken into account.⁸

The effects of the rates of the main elementary steps, namely, CO and NO diffusion and desorption, NO dissociation, N_2 production through the formation of the $(\text{N}-\text{NO})^*$ intermediary species, and the classical $\text{N} + \text{N}$ recombination, phase transformations, and the behavior of the oscillation period under temperature changes, have been investigated in detail with the following principal results:

(a) Sustained oscillations can only be observed if a synchronized mechanism is achieved and also if cellular spatial patterns are formed. On the other hand, when irregular, modulated, and damped oscillations are observed, the synchronization is always removed and cellular structures decay in turbulent spatial behavior, which is maintained indefinitely. Experimentally, the oscillatory behavior is associated with spatial pattern formation in a similar way.¹

(b) On large grids (512×512 cells or greater), sustained oscillations appear if NO and CO diffusion rates are relatively high (30 s^{-1} or more), and if these rates values increase, the oscillation period become longer. The same effect is observed if CO diffusion is larger than that of NO diffusion.

(c) CO and NO diffusions have the same importance, because if any of these processes is neglected, then oscillations are not observed in the system.

(d) Modulated oscillations appear in our study when the NO diffusion rate is larger than that of CO, increasing in this way the effective NO dissociation rate.

(e) CO and NO desorption rates need to be tuned to rather low values for sustained oscillations. If these rates have intermediate values, between 1×10^{-4} and $1 \times 10^{-2} \text{ s}^{-1}$, then the oscillation periods have a regular behavior for high NO and CO diffusion rates. If the NO and CO diffusion have low values (10 s^{-1}) and the desorption rates are in the intermediate range, then the sustained oscillations decline in favor of damped oscillations. If the desorption rates increase even more, then irregular oscillations are generated.

(f) When initial NO dissociation rate is increased, the periods of the sustained oscillations become shorter; if this rate increases even more, modulated oscillations are observed at high diffusion of both molecules CO and NO. If this initial rate decreases, the oscillation periods are larger. The effect of N-islands formation is of little importance on the behavior of the system, perhaps because only small islands are formed due to the dynamics of the reaction, and so is the effect of NO dissociation enhancement due to the presence of nn vacant sites. However, it is found that the inhibition effect on NO dissociation due to the presence of coadsorbed nn NO or CO is of crucial importance. This inhibition effect, on the other hand, is also responsible for the formation of NO/CO islands which are essential to the building up of the oscillatory behavior.

(g) When the classical $\text{N} + \text{N}$ recombination step is eliminated, all reported phenomena are again observed in the system, but if the $(\text{N}-\text{NO})^*$ intermediary complex pathway is neglected, the system shows only damped oscillations and turbulent patterns. Therefore the $(\text{N}-\text{NO})^*$ pathway is more important than the $\text{N} + \text{N}$ recombination one in producing N_2 in the reaction.

(h) Oscillation frequency increases (oscillation period decreases) when the temperature is increased, in qualitative concordance with experimental observations.

It is important to note that the length scales for simulated and experimentally observed patterns are very different. In our simulations a lattice size of 1024 cells represents a real length of approximately $0.28 \mu\text{m}$, while patterns have been observed experimentally on surfaces whose size ranges from 30 to $500 \mu\text{m}$. In addition, as mentioned above, the synchronization mechanism is also based on different phenomena: While in experiments at high T , synchronization is most likely achieved via global coupling through the gas phase; in simulations it is achieved through the rapid diffusion of adsorbed species. Therefore, comparisons between simulations and experiments should be carried out with care and in any case they can only be of a qualitative nature. Among the patterns reported in these simulations, turbulent patterns in the $\text{NO} + \text{CO}$ reaction have been reported experimentally in refs 3 and 4 and bubble patterns have been reported in the $\text{CO} + \text{O}_2$ reaction in ref 47. We have not observed other kinds of patterns, such as parallel wave trains and spiral waves, which have been observed experimentally in refs 3 and 4.

In summary, we have developed a model which includes experimental information about detailed elementary reaction steps for the reduction of NO by CO on a Pt(100) surface. This model reveals many features observed in catalytic reactions on this single crystal or inclusive on other single-crystal surfaces.

Acknowledgment. Financial support and scholarship to S. de Jesús Alas G. from Consejo Nacional de Ciencia y Tecnología (CONACyT, México) is gratefully acknowledged. The authors are grateful for the support of CONACyT-CONICET through the cooperation project "Catálisis, Fisicoquímica de Superficies e Interfases Gas-Sólido" between México and Argentina.

References and Notes

- (1) Vesper, G.; Imbihl, R. *J. Chem. Phys.* **1992**, *96*, 7155.
- (2) Schwartz, S. B.; Schmidt, L. D. *Surf. Sci.* **1988**, *206*, 169.
- (3) Vesper, G.; Mertens, F.; Mikhailov, A. S.; Imbihl, R. *Phys. Rev. Lett.* **1993**, *71*, 935.
- (4) Vesper, G.; Imbihl, R. *J. Chem. Phys.* **1994**, *100*, 8483; **1994**, *100*, 8492.
- (5) Imbihl, R.; Ertl, G. *Chem. Rev.* **1995**, *95*, 697.
- (6) Fink, Th.; Dath, J.-P.; Imbihl, R.; Ertl, G. *J. Chem. Phys.* **1991**, *95*, 2109.
- (7) Khrustova, N.; Vesper, G.; Mikhailov, A.; Imbihl, R. *Phys. Rev. Lett.* **1995**, *75*, 3564.
- (8) Zhdanov, V. P. *J. Chem. Phys.* **1999**, *110*, 8748.
- (9) Fink, Th.; Dath, J.-P.; Imbihl, R.; Ertl, G. *Surf. Sci.* **1991**, *251*, 985.
- (10) Fink, Th.; Dath, J.-P.; Bassett, M. R.; Imbihl, R.; Ertl, G. *Surf. Sci.* **1991**, *245*, 96.
- (11) Hartmann, N.; Kevrekidis, Y.; Imbihl, R. *J. Chem. Phys.* **2000**, *112*, 6795.
- (12) Meng, B.; Weinberg, W. H.; Evans, J. W. *J. Chem. Phys.* **1994**, *101*, 3234.
- (13) Tammaro, M.; Evans, J. W. *J. Chem. Phys.* **1998**, *108*, 7795.
- (14) Kortlüke, O.; Kuzovkov, V. N.; von Niessen, W. *Phys. Rev. Lett.* **1998**, *81*, 2164.
- (15) Zhdanov, V. P.; Kasemo, B. *Surf. Sci. Rep.* **1997**, *29*, 31.
- (16) Zaera, F.; Gopinath, C. S. *J. Chem. Phys.* **1999**, *111*, 8088.
- (17) Zaera, F.; Gopinath, C. S. *Chem. Phys. Lett.* **2000**, *332*, 209.
- (18) Gopinath, C. S.; Zaera, F. *J. Phys. Chem. B* **2000**, *104*, 3194.
- (19) Zaera, F.; Wehner, S.; Gopinath, C. S.; Sales, J. L.; Gargiulo, V.; Zgrablich, G. *J. Phys. Chem. B* **2000**, *105*, 7771.
- (20) Bustos, V.; Gopinath, C. S.; Uñac, R.; Zaera, F.; Zgrablich, G. *J. Chem. Phys.* **2001**, *114*, 10927.
- (21) Zaera, F.; Gopinath, C. S. *J. Chem. Phys.* **2002**, *116*, 1128.
- (22) Zaera, F.; Gopinath, C. S. *Phys. Chem. Chem. Phys.* **2003**, *5*, 646.
- (23) Avalos, L. A.; Bustos, V.; Uñac, R.; Zaera, F.; Zgrablich, G. *J. Mol. Catal. A: Chem.* **2005**, *228*, 89.
- (24) Alas, S. J.; Cordero, S.; Kornhauser, I.; Zgrablich, G. *J. Chem. Phys.* **2005**, *122*, 144705.
- (25) Alas, S. J.; Rojas, F.; Kornhauser, I.; Zgrablich, G. *J. Mol. Catal. A: Chem.* **2006**, *244*, 183.
- (26) Kortlüke, O.; Von Niessen, W. *J. Chem. Phys.* **1996**, *105*, 4764.
- (27) Cho, B. K. *J. Catal.* **1992**, *138*, 255.
- (28) Hecker, W. C.; Bell, A. T. *J. Catal.* **1983**, *84*, 200.
- (29) Mei, D.; Ge, Q.; Neurock, M.; Kieken, L.; Lerou, J. *Mol. Phys.* **2004**, *102*, 361.
- (30) Neurock, M.; Wasileski, S. A.; Mei, D. *Chem. Eng. Sci.* **2004**, *59*, 4703.
- (31) Borg, H. J.; Reijerse, J. F. C.-J. M.; van Santen, R. A.; Niemantsverdriet, J. W. *J. Chem. Phys.* **1994**, *101*, 10052.
- (32) Binder, K. *Monte Carlo Methods in Statistical Physics*; Springer: Berlin, 1986.
- (33) Behm, R. J.; Thiel, P. A.; Norton, P. R.; Ertl, G. *J. Chem. Phys.* **1983**, *78*, 7437; **1983**, *78*, 7448.
- (34) Barteau, M. A.; Ko, E. I.; Madix, R. J. *Surf. Sci.* **1981**, *102*, 99.
- (35) Mase, K.; Murata, Y. *Surf. Sci.* **1992**, *277*, 97.
- (36) Yeo, Y. Y.; Vattuone, L.; King, D. A. *J. Chem. Phys.* **1996**, *104*, 3810.
- (37) Norton, P. R.; Griffiths, K.; Binder, P. E. *Surf. Sci.* **1984**, *138*, 125.
- (38) Gelten, R. J.; Jansen, A. P. J.; van Santen, R. A.; Lukkien, J. J.; Segers, J. P. L.; Hilbers, P. A. J. *J. Chem. Phys.* **1998**, *108*, 5921.
- (39) Lukkien, J. J.; Segers, J. P. L.; Hilbers, P. A. J.; Gelten, R. J.; Jansen, A. P. *J. Phys. Rev. E* **1998**, *58*, 2598.
- (40) van Kampen, N. G. *Stochastic Processes in Physics and Chemistry*; North-Holland: Amsterdam, 1992.
- (41) Hinrichsen, H. *Adv. Phys.* **2000**, *49*, 815.
- (42) There are no theoretical or experimental arguments supporting this hypothesis for Pt(100). This effect is included here only on the basis of the observed behavior for Rh(111). Simulations will finally show that the effect is negligible, since N-islands do not grow due to the rapid consumption of N species on the surface.
- (43) Yeo, Y. Y.; Wartnaby, C. E.; King, D. A. *Science* **1995**, *268*, 1731.
- (44) Jackman, T. E.; Griffiths, K.; Davies, J. A.; Norton, P. R. *J. Chem. Phys.* **1983**, *79*, 3529.
- (45) Thiel, P. A.; Behm, R. J.; Norton, P. R.; Ertl, G. *Surf. Sci.* **1982**, *121*, L553.
- (46) Hopkinson, A.; Bradley, J. M.; Guo, X. C.; King, D. A. *Phys. Rev. Lett.* **1993**, *71*, 1597.
- (47) Rose, K. C.; Battogtokh, D.; Mikhailov, A.; Imbihl, R.; Engel, W.; Bradshaw, A. M. *Phys. Rev. Lett.* **1996**, *76*, 3582.
- (48) Ross, J.; Vlad, M. O. *Annu. Rev. Phys. Chem.* **1999**, *50*, 51.